ISME

Three-Dimensional Elasticity Solution of Single Layer Piezoelectric Panel

M. Shakeri *
Professor

M.R. Sedighi †
Ph.D student

A.R. Daneshmehr ‡
Assistant professor

This research presents a semi analytical solution of finitely long, simply supported, orthotropic, piezoelectric, radially polarized, shell panel under pressure and electrostatic excitation. The general solution of the governing partial differential equations are obtained by the method of separation of variables. The displacements and electric potential are expanded in appropriate trigonometric Fourier series in the circumferential and axial coordinate to satisfy the boundary conditions at the simply-supported circumferential and axial edges. The governing ordinary differential equations are solved by the Galerkin finite element method. In this procedure, the quadratic shape function is used in each element. Numerical examples are provided for typical external pressure on outer surface of a single layer piezoelectric panel.

Keyword: linear piezoelectric, finitely long, cylindrical panel, orthotropic, radially polarized, simply-supported

1 Introduction

The coupling effect existing between the elastic and electric fields in piezoelectric materials is used in various engineering applications. The direct piezoeffect is used in sensors in electromechanical transducers to measure the deformation from the induced electrical potential difference. The inverse piezoeffect is used in electromechanical actuators for controlling an entity by the application of appropriate electrical potential differences. The piezoelectric materials have enormous potential for use as distributed actuators and sensors for active control of smart structural systems [1]. Very few exact solutions of the three-dimensional field equations are available for coupled response of piezoelectric elements to electromechanical loading. These analytical solutions are needed to assess the accuracy of the various two-dimensional plate and shell theory formulations [2].

Exact analytical solutions have been presented for the direct and inverse piezoelastic problems of infinitely long, simply-supported, cylindrically orthotropic circular cylindrical panel in cylindrical bending under pressure and electrostatic excitation. Detailed results have been presented for sinusoidal, uniform and patch loadings [2]. Ray *et al.* [3, 4] presented exact solution for static analysis of a simply-supported piezoelectric flat panel and a layered intelligent flat

*Corresponding author, Dept. of Mech. Eng., Amirkabir Univ. of Tech., Tehran, Iran, E-mail: shakeri@aut.ac.ir
†Dept. of Mech. Eng., Amirkabir Univ. of Tech., Tehran, Iran
‡Dept. of Mech. Eng., Industrial Faculty, Islamic Azad Univ., Central Tehran Branch, Tehran, Iran

panel under cylindrical bending. Three-dimensional exact analysis of simply-supported rectangular plate coupled with distributed sensors and actuators have been presented by Ray *et al.* [5]. Mitchell and Reddy [6] have presented a power series solution for static analysis of an axisymmetric problem of axial loading on a composite cylinder with surfacebonded or embedded piezoelectric laminae. Ren [7]has presented the exact elasticity solution of simply-supported laminated circular cylindrical panels in cylindrical bending. Exact solution of orthotropic cylindrical shell with piezoelectric layer under cylindrical bending have been studied by Chen *et al.* [8]. Also, the piezoelastic solution of infinitely long cylindrical panel and shell structures is presented by Kapuria *et al.* in [9]. Shakeri *et al.* have presented elasticity solution of finitely long, simply-supported, orthotropic, piezoelectric shell panel under pressure and electrostatic excitation [10], and elastic solution of orthotropic thick laminated cylindrical panels under dynamic loading [11].

In this work we present a semi analytical solution of a finitely long, simply supported, orthotropic, piezoelectric, radially polarized, circular cylindrical shell panel under pressure, where panel is closed circuit. The general solution of the governing differential equations is obtained by the method of separation of variables. The displacements and electric potential are expanded in appropriate trigonometric Fourier series in the circumferential and axial coordinates to satisfy the boundary conditions at the simply-supported circumferential and axial ends. The prescribed electromechanical functions on lateral boundary are expanded in term of the trigonometric Fourier series along the circumferential and axial coordinate. The highly coupled partial differential equation (P.D.E) are reduced to ordinary differential equations (O.D.E) with variable coefficients by trigonometric function expansion in circumferential and axial directions. The resulting ordinary differential equation are solved by the Galerkin finite element method. In this method, we used quadratic element instead of the linear one.

2 Governing equations

The linear constitutive equations of a piezoelectric medium are given by

$$\{\sigma\} = [C]\ \{\varepsilon\} - [e]^T\ \{E\}, \qquad \{D\} = [e]\ \{\varepsilon\} + [\eta]\ \{E\} \tag{1}$$

where the stress components $\{\sigma\}$, the strain components $\{\varepsilon\}$, the electric field vector $\{E\}$ and the electric displacement vector $\{D\}$ are given in cylindrical coordinate system (r, θ, z) by

$$\{\sigma\} = \left[\ \sigma_{rr} \quad \sigma_{\theta\theta} \quad \sigma_{zz} \quad \tau_{\theta z} \quad \tau_{rz} \quad \tau_{r\theta}\ \right]^T, \quad \{E\} = \left[\ E_r \quad E_\theta \quad E_z\ \right]^T \tag{2}$$

$$\{\varepsilon\} = \left[\ \varepsilon_{rr} \quad \varepsilon_{\theta\theta} \quad \varepsilon_{zz} \quad \gamma_{\theta z} \quad \gamma_{rz} \quad \gamma_{r\theta}\ \right]^T, \quad \{D\} = \left[\ D_r \quad D_\theta \quad D_z\ \right]^T \tag{3}$$

Here, $[C]$, $[e]$, $[\eta]$ denote, respectively, the matrices of elastic constants, piezoelectric constants and dielectric constants of the piezoelastic material. The equation of equilibrium in the absence of body force and the charge equation of equilibrium of electrostatic in cylindrical coordinate system are

$$\frac{\partial \sigma_{rr}}{\partial r} + \frac{\sigma_{rr} - \sigma_{\theta\theta}}{r} + \frac{1}{r}\frac{\partial \tau_{r\theta}}{\partial \theta} + \frac{\partial \tau_{rz}}{\partial z} = 0 \tag{4}$$

$$\frac{\partial \tau_{r\theta}}{\partial r} + \frac{1}{r}\frac{\partial \sigma_{\theta\theta}}{\partial \theta} + \frac{\partial \tau_{\theta z}}{\partial z} + 2\,\frac{\tau_{r\theta}}{r} = 0 \tag{5}$$

$$\frac{\partial \tau_{rz}}{\partial r} + \frac{1}{r}\,\frac{\partial \tau_{\theta z}}{\partial \theta} + \frac{\partial \sigma_{zz}}{\partial z} + \frac{\tau_{rz}}{r} = 0 \tag{6}$$

$$\frac{1}{r}\frac{\partial\, r\, D_r}{\partial r} + \frac{1}{r}\frac{\partial D_\theta}{\partial \theta} + \frac{\partial D_z}{\partial z} = 0 \tag{7}$$

We consider a cylindrically orthotropic piezoelectric material with poling in **lateral (radial)** direction . The matrices $[C]$, $[e]$ and $[\eta]$, as given by Tiersten [12], are

$$[C]=\begin{bmatrix} C_{11} & C_{12} & C_{13} & 0 & 0 & 0 \\ C_{12} & C_{22} & C_{23} & 0 & 0 & 0 \\ C_{13} & C_{23} & C_{33} & 0 & 0 & 0 \\ 0 & 0 & 0 & C_{44} & 0 & 0 \\ 0 & 0 & 0 & 0 & C_{55} & 0 \\ 0 & 0 & 0 & 0 & 0 & C_{66} \end{bmatrix} \tag{8}$$

$$[e]=\begin{bmatrix} e_{33} & e_{32} & e_{31} & 0 & 0 & 0 \\ 0 & 0 & 0 & 0 & 0 & e_{24} \\ 0 & 0 & 0 & 0 & e_{15} & 0 \end{bmatrix}, \quad [\eta]=\begin{bmatrix} \eta_{33} & 0 & 0 \\ 0 & \eta_{11} & 0 \\ 0 & 0 & \eta_{22} \end{bmatrix}$$

Using relations (8), the constitutive equations (1) can be written as

$$\begin{aligned} \sigma_{rr} &= C_{11}\varepsilon_{rr} + C_{12}\varepsilon_{\theta\theta} + C_{13}\varepsilon_{zz} - e_{33}E_r \\ \sigma_{\theta\theta} &= C_{12}\varepsilon_{rr} + C_{22}\varepsilon_{\theta\theta} + C_{23}\varepsilon_{zz} - e_{32}\,E_r \\ \sigma_{zz} &= C_{13}\varepsilon_{rr} + C_{23}\varepsilon_{\theta\theta} + C_{33}\varepsilon_{zz} - e_{31}\,E_r \\ \tau_{\theta z} &= C_{44}\gamma_{\theta z} \\ \tau_{rz} &= C_{55}\gamma_{rz} - e_{15}\,E_z \\ \tau_{r\theta} &= C_{66}\gamma_{r\theta} - e_{24}\,E_\theta \end{aligned} \tag{9}$$

and

$$\begin{aligned} D_r &= e_{33}\,\varepsilon_{rr} + e_{32}\,\varepsilon_\theta + e_{31}\,\varepsilon_z + \eta_{33}\,E_r \\ D_\theta &= e_{24}\,\gamma_{r\theta} + \eta_{22}\,E_\theta \\ D_z &= e_{15}\gamma_{rz} + \eta_{11}\,E_z \end{aligned} \tag{10}$$

Consider a finite circular cylindrical shell panel of mean radius R_m, thickness H, length L and angular span α, as shown in Fig.1. Its longitudinal and circumferential ends are simply-supported and electrically grounded at $z=(0,L)$ and $\theta=(0,\alpha)$, respectively. Its lateral surfaces at $r=R_a=R_m-H/2$ and $r=R_b=R_m+H/2$ are subjected to electrical and traction excitations which vary along the longitudinal (z) and circumferential (θ) directions.

The strains are related to the radial, circumferential and axial displacement components u_r, u_θ and u_z by

$$\varepsilon_{rr}=\frac{\partial u_r}{\partial r} \quad , \quad \varepsilon_{\theta\theta}=\frac{1}{r}\left(u_r+\frac{\partial u_\theta}{\partial \theta}\right) \quad , \quad \varepsilon_z=\frac{\partial u_z}{\partial z} \tag{11}$$

$$\gamma_{\theta z}=\frac{\partial u_\theta}{\partial z}+\frac{1}{r}\frac{\partial u_z}{\partial \theta} \quad , \quad \gamma_{rz}=\frac{\partial u_z}{\partial r}+\frac{\partial u_r}{\partial z} \quad , \quad \gamma_{r\theta}=\frac{1}{r}\left(\frac{\partial u_r}{\partial \theta}-u_\theta+r\frac{\partial u_\theta}{\partial r}\right)$$

The electric field is related to the electrical potential, ψ, of the piezoelectric medium by

$$E_r=-\frac{\partial \psi}{\partial r} \quad , \quad E_\theta=-\frac{1}{r}\frac{\partial \psi}{\partial \theta} \quad , \quad E_z=-\frac{\partial \psi}{\partial z} \tag{12}$$

Using equations (9)-(12), the partial differential equations of motion (i.e. equations (4)-(7)) can be expressed to Navier form. Thus, the Navier form of equations of motion can be written in operator form as

$$\begin{bmatrix} L_{1r} & L_{1\theta} & L_{1z} & L_{1\psi} \\ L_{2r} & L_{2\theta} & L_{2z} & L_{2\psi} \\ L_{3r} & L_{3\theta} & L_{3z} & L_{3\psi} \\ L_{4r} & L_{4\theta} & L_{4z} & L_{4\psi} \end{bmatrix} \begin{Bmatrix} u_r \\ u_\theta \\ u_z \\ \psi \end{Bmatrix} = \begin{Bmatrix} 0 \\ 0 \\ 0 \\ 0 \end{Bmatrix} \tag{13}$$

where L_{ij}, are given in appendix A, where $i = 1, 2, 3, 4$ and $j = r, \theta, z, \psi$.

Let the prescribed pressure and electrical potential or electrical displacement D_r to cause actuation strain at the inner and outer surfaces be $p_a(\theta, z),\ \psi_a(\theta, z)$ or $D_a(\theta, z)$ and $p_b(\theta, z),\ \psi_b(\theta, z)$ or $D_b(\theta, z)$, respectively. Boundary conditions at the axial ends at $z = 0,\ L$ are :

$$\begin{aligned} u_r(r,\theta,0) &= u_r(r,\theta,L) = 0 \\ \sigma_{zz}(r,\theta,0) &= \sigma_{zz}(r,\theta,L) = 0 \\ \tau_{r\theta}(r,\theta,0) &= \tau_{r\theta}(r,\theta,L) = 0 \\ \psi(r,\theta,0) &= \psi(r,\theta,L) = 0 \end{aligned} \tag{14}$$

Boundary conditions at the circumferential ends at $\theta = 0,\ \alpha$ are :

$$\begin{aligned} u_r(r,0,z) &= u_r(r,\alpha,z) = 0 \\ \sigma_{\theta\theta}(r,0,z) &= \sigma_{\theta\theta}(r,\alpha,z) = 0 \\ \tau_{rz}(r,0,z) &= \tau_{rz}(r,\alpha,z) = 0 \\ \psi(r,0,z) &= \psi(r,\alpha,z) = 0 \end{aligned} \tag{15}$$

In the the lateral surfaces at $r = R_a,\ R_b$ the boundary conditions are :

$$\begin{aligned} &\sigma_{rr}(R_a,\theta,z) = -p_a(\theta,z), && \sigma_{rr}(R_b,\theta,z) = -p_b(\theta,z) \\ &\tau_{r\theta}(R_a,\theta,z) = 0, && \tau_{r\theta}(R_b,\theta,z) = 0 \\ &\psi(R_a,\theta,z) = \psi_a(\theta,z), && \psi(R_b,\theta,z) = \psi_b(\theta,z) \\ &\qquad or && \qquad or \\ &D_r(R_a,\theta,z) = D_a(\theta,z), && D_r(R_b,\theta,z) = D_b(\theta,z) \end{aligned} \tag{16}$$

3 General solution of the governing equations

The solution of the boundary value problem, satisfying the boundary conditions (14) and (15), is taken in the following separable form:

$$\begin{aligned} u_r &= \sum_{m=1}^{\infty}\sum_{n=1}^{\infty} \phi_r(r)\ \sin(b_m\theta)\sin(b_n z) \\ u_\theta &= \sum_{m=1}^{\infty}\sum_{n=1}^{\infty} \phi_\theta(r)\ \cos(b_m\theta)\sin(b_n z) \\ u_z &= \sum_{m=1}^{\infty}\sum_{n=1}^{\infty} \phi_z(r)\ \sin(b_m\theta)\cos(b_n z) \\ \psi &= \sum_{m=1}^{\infty}\sum_{n=1}^{\infty} \phi_\psi(r)\ \sin(b_m\theta)\sin(b_n z) \end{aligned} \tag{17}$$

where $b_m = m\pi/\alpha$ and $b_n = n\pi/L$. Using equations (13) and (17), the partial differential equations of motion (Navier equations) will be reduced to ordinary differential equations. These ordinary differential equations can be written in operator form as

$$\begin{bmatrix} L^*_{1r} & L^*_{1\theta} & L^*_{1z} & L^*_{1\psi} \\ L^*_{2r} & L^*_{2\theta} & L^*_{2z} & L^*_{2\psi} \\ L^*_{3r} & L^*_{3\theta} & L^*_{3z} & L^*_{3\psi} \\ L^*_{4r} & L^*_{4\theta} & L^*_{4z} & L^*_{4\psi} \end{bmatrix} \begin{Bmatrix} \phi_r(r) \\ \phi_\theta(r) \\ \phi_z(r) \\ \phi_\psi(r) \end{Bmatrix} = \begin{Bmatrix} 0 \\ 0 \\ 0 \\ 0 \end{Bmatrix} \tag{18}$$

where L^*_{ij} are given in appendix A, where $i = 1,2,3,4$ and $j = r,\theta,z,\psi$. These system of equations are solved by the Galerkin finite element method. The quadratic shape functions N_i, N_j and N_k are considered for ϕ_r,ϕ_θ, ϕ_z and ϕ_ψ,

$$\phi_s = \begin{bmatrix} N_i & N_j & N_k \end{bmatrix} \begin{Bmatrix} \phi_{si} \\ \phi_{sj} \\ \phi_{sk} \end{Bmatrix}, \quad s = r,\theta,z,\psi \tag{19}$$

where N_i, N_j and N_k are :

$$N_i(r) = \frac{(r-r_k)\,(2\,r-r_k-r_i)}{(r_k-r_i)^2}$$
$$N_j(r) = 4\frac{(r_k-r)(r-r_i)}{(r_k-r_i)^2}$$
$$N_k(r) = \frac{(r-r_i)\,(2\,r-r_k-r_i)}{(r_k-r_i)^2}$$

After multiplying the first of Eq.(18) by N_i and one time part by part integration of the second order differential terms, the weak form of equation is obtained. By integrating this equation we obtain an algebraic equation in the form

$$\begin{aligned} &A_1\phi_{ir} + A_2\phi_{i\theta} + A_3\phi_{iz} + A_4\phi_{i\psi} + \\ &A_5\phi_{jr} + A_6\phi_{j\theta} + A_7\phi_{jz} + A_8\phi_{j\psi} + A_9\phi_{kr} + A_{10}\phi_{k\theta} + A_{11}\phi_{kz} + A_{12}\phi_{k\psi} = F_1 \end{aligned} \tag{20}$$

By integrating the other ordinary differential equations given by Eq.(18), three equations similar to equation (20) are obtained. Repeating the above procedure by N_j and N_k instead of N_i, give another eight equations. Rewriting these twelve equations in form of matrix equations, we obtain the following finite element equilibrium equation for each non-boundary elements:

$$[K]_e\{X\}_e = \{F\}_e \tag{21}$$

where $[K]_{12\times12}$ and $\{F\}_{12\times1}$ are the stiffness and force matrices, respectively, and :

$$\{X\}_e^T = \{\phi_{ri}\ \ \phi_{\theta i}\ \ \phi_{zi}\ \ \phi_{\psi i}\ \ \phi_{rj}\ \ \phi_{\theta j}\ \ \phi_{zj}\ \ \phi_{\psi j}\ \ \phi_{rk}\ \ \phi_{\theta k}\ \ \phi_{zk}\ \ \phi_{\psi k}\}$$

Applying the boundary conditions (16) to the first and last nodes in the medium i.e. two lateral surfaces and using the equations (19), the displacement value of these nodes are given by:

$$\begin{aligned} \phi_{r1} &= C_1\phi_{r2} + C_2\phi_{\theta2} + C_3\phi_{z2} + C_4\phi_{\psi2} + C_5\phi_{r3} + C_6\phi_{\theta3} + C_7\phi_{z3} + C_8\phi_{\psi3} \\ \phi_{\theta1} &= C_1'\phi_{r2} + C_2'\phi_{\theta2} + C_3'\phi_{z2} + C_4'\phi_{\psi2} + C_5'\phi_{r3} + C_6'\phi_{\theta3} + C_7'\phi_{z3} + C_8'\phi_{\psi3} \\ \phi_{z1} &= C_1''\phi_{r2} + C_2''\phi_{\theta2} + C_3''\phi_{z2} + C_4''\phi_{\psi2} + C_5''\phi_{r3} + C_6''\phi_{\theta3} + C_7''\phi_{z3} + C_8''\phi_{\psi3} \\ \phi_{\psi1} &= C_1'''\phi_{r2} + C_2'''\phi_{\theta2} + C_3'''\phi_{z2} + C_4'''\phi_{\psi2} + C_5'''\phi_{r3} + C_6'''\phi_{\theta3} + C_7'''\phi_{z3} + C_8'''\phi_{\psi3} \end{aligned} \tag{22}$$

$$\begin{aligned} \phi_{rML} &= D_1\phi_{r(ML-2)} + D_2\phi_{\theta(ML-2)} + D_3\phi_{z(ML-2)} + D_4\phi_{\psi(ML-2)} \\ &+ D_5\phi_{r(ML-1)} + D_6\phi_{\theta(ML-1)} + D_7\phi_{z(ML-1)} + D_8\phi_{\psi(ML-1)} \\ \phi_{\theta ML} &= D_1'\phi_{r(ML-2)} + D_2'\phi_{\theta(ML-2)} + D_3'\phi_{z(ML-2)} + D_4'\phi_{\psi(ML-2)} \\ &+ D_5'\phi_{r(ML-1)} + D_6'\phi_{\theta(ML-1)} + D_7'\phi_{z(ML-1)} + D_8'\phi_{\psi(ML-1)} \\ \phi_{zML} &= D_1''\phi_{r(ML-2)} + D_2''\phi_{\theta(ML-2)} + D_3''\phi_{z(ML-2)} + D_4''\phi_{\psi(ML-2)} \\ &+ D_5''\phi_{r(ML-1)} + D_6''\phi_{\theta(ML-1)} + D_7''\phi_{z(ML-1)} + D_8''\phi_{\psi(ML-1)} \\ \phi_{\psi ML} &= D_1'''\phi_{r(ML-2)} + D_2'''\phi_{\theta(ML-2)} + D_3'''\phi_{z(ML-2)} + D_4'''\phi_{\psi(ML-2)} \\ &+ D_5'''\phi_{r(ML-1)} + D_6'''\phi_{\theta(ML-1)} + D_7'''\phi_{z(ML-1)} + D_8'''\phi_{\psi(ML-1)} \end{aligned} \tag{23}$$

where $C_1, ...C_8'''$, $D_1', ...D_8'''$ are constants. By substituting equations (22) and (23) into (21), the finite element equilibrium equations for the first and last elements become :

$$[K]_1\{X\}_1 = \{F\}_1, \qquad [K]_{ML}\{X\}_{ML} = \{F\}_{ML} \tag{24}$$

Assembling equations (21) and (24), the global finite element equilibrium equation is obtained as :

$$[K]\{X\} = \{F\} \tag{25}$$

Once the finite element equilibrium is established, we can solve this set of algebric equations for unknown $\{X\}$ vector. Here, this system of equations is solved using the *LinearSolve* procedure of *Maple*.

4 Numerical results

Here, to verify the results, consider a panel with span angle $\alpha = \pi/3$, and $L = 4R_m$,(R_m is mean radius of panel) that is polarized in radial direction and subjected to the following electromechanical loads.

$$\psi_a(\theta, z) = \psi_b(\theta, z) = 0, \;\; p_a(\theta, z) = 0, \;\; p_b(\theta, z) = p_0 \sin(\pi\theta/\alpha)\sin(\pi z/L)$$

The piezoelectric material considered here is elastically orthotropic. The material properties of piezoelectric are given in the Table (1). The numerical results are expressed in dimensionless

Modulii	PZT4	Unit
C_{11}	113	GPa
C_{22}	139	GPa
C_{33}	139	GPa
C_{44}	2.6	GPa
C_{55}	25.6	GPa
C_{66}	25.6	GPa
C_{12}	74.3	GPa
C_{13}	74.3	GPa
C_{23}	77.8	GPa
e_{15}	12.7	C/m^2
e_{24}	12.7	C/m^2
e_{31}	-5.2	C/m^2
e_{32}	-5.2	C/m^2
e_{33}	15.1	C/m^2
η_{11}	6.46	$\mu F/m$
η_{22}	6.46	$\mu F/m$
η_{33}	5.62	$\mu F/m$

Table 1 Elastic, piezoelectric and dielectric properties of PZT4

form as follows :

$$(\tilde{u}_r, \tilde{u}_\theta, \tilde{u}_z) = \frac{100Y}{HS^4 p_0}(u_r, u_\theta, u_z), \qquad \tilde{\psi} = \frac{|d|Y}{HS^4 p_0}\psi \tag{26}$$

$$\tilde{\sigma}_r = \frac{\sigma_r}{p_0}, \qquad (\tilde{\sigma}_\theta, \tilde{\sigma}_z) = \frac{(\sigma_\theta, \sigma_z)}{S^2 p_0}, \qquad (\tilde{\tau}_{\theta z}, \tilde{\tau}_{rz}, \tilde{\tau}_{r\theta}) = \frac{(\tau_{\theta z}, \tau_{rz}, \tau_{r\theta})}{S p_0} \tag{27}$$

where Y and d denote the Young's modulus and the piezoelectric coefficient in the radial direction, respectively, and :

$$S = R_m/H\,, \quad H = R_b - R_a\,, \quad ;\; R_m = (R_a + R_b)/2\,, \quad p_0 = 1.$$

Here, the direct effects of piezoelectric is considered. In this case, panel is subjected to only mechanical loading. Sinusoidal pressure loading is applied to the outer surface of the panel, where both its lateral surfaces are held at zero potential. Since the mechanical pressure loading is sinusoidal, only one term of the Fourier series is needed to be considered. Figures (2)-(10) illustrate various entities at locations where they are high. The variation across the thickness $[\zeta = (r - R_m)/H]$ of the displacements $\tilde{u}_r$ at $(\theta = \alpha/2, z = L/2)$ and $\tilde{u}_\theta$ at $(\theta = 0, z = L/2)$ are depicted in figures (2) and (3) for $S = 4$, respectively. These figures obviously show that the distribution of $\tilde{u}_r$ across the thickness is parabolic form and variation of $\tilde{u}_\theta$ through the thickness is approximately linear.

The variations across the thickness of electrical potential ψ at $(\theta = \alpha/2, z = L/2)$ is shown in Fig. (4). This figure shows that electrical potential distribution through the thickness is very close to parabola form.

The distributions across the thickness of $\tilde{\sigma}_{rr}$, $\tilde{\sigma}_{\theta\theta}$ and $\tilde{\sigma}_{zz}$ at $(\theta = \alpha/2, z = L/2)$ are illustrated in Figs. (5)-(7). In these figures we can find that distribution of $\tilde{\sigma}_{rr}$ from the inner surface up to mean radius R_m is parabolic and between R_m and the outer surface is linear and distributions of $\tilde{\sigma}_{\theta\theta}$ and $\tilde{\sigma}_{zz}$ are linear. In all of the above figures the boundary conditions are satisfied.

The distribution of shear stress $\tilde{\tau}_{\theta z}$ through the thickness at $(\theta = 0, z = L)$ is shown in Fig. (8).This figure shows that variation through thickness of shear stress $\tilde{\tau}_{\theta z}$ is linear.

Similarly, the distribution of shear stress $\tilde{\tau}_{rz}$ through the thickness at $(\theta = \alpha/2, z = L)$ is shown in Fig. (9). The distribution across the thickness of in-plane shear stress $\tilde{\tau}_{r\theta}$ at $(\theta = 0, z = L/2)$ is depicted in Fig. (10). These two last figure show the distribution of shear stresses $\tilde{\tau}_{rz}$ and $\tilde{\tau}_{r\theta}$ through the thickness are parabolic.

5 Conclusion

In this work we present a semianalytical solution of a finitely long, simply-supported, orthotropic, piezoelectric, radially polarized, circular cylindrical shell panel under pressure, where panel is closed circuit. The general solution of the governing differential equations is obtained by the method of separation of variables. The displacements and electric potential are expanded in the appropriate trigonometric Fourier series in the circumferential and axial coordinates to satisfy the boundary conditions at the simply-supported circumferential and axial ends. The prescribed electromechanical functions on lateral boundaries are expanded in terms of the trigonometric Fourier series in the circumferential and axial coordinates. The highly coupled partial differential equation (P.D.E) are reduced to ordinary differential equations (O.D.E) with variable coefficients by trigonometric function expansion in circumferential and axial directions. The resulting ordinary differential equation are solved by the Galerkin finite element method. In this method, we used the quadratic element instead of the linear ones.

It is always assumed in the analytical analysis (two-dimensional plate and shell theory) of the piezoelectric structures that the electric potential in the the piezoeletric layers varied linearly and the displacements change in the form of prescribed functions across its thickness [13]. However,

it has been shown that the distributions of the mechanical displacement and electric potential of piezoelectric are very complicated and cannot be treated as pure elastic structures. Therefore, three-dimensional analysis of piezoelectric structures is recommended even for thin structures. Since a comprehensive and exact study of active piezoelectric structure is still unavailable, the present work provides an enhanced insight to the mechanical and electrical behavior of this type of smart structures. Results of this paper are also useful for assessing approximate analysis.

References

[1] Crawley, F.E., “Intelligent Structures for Aerospace: A Technology Overview and Assessment”, AIAA J., Vol. 32, pp. 1689-1700, (1994).

[2] Dumir, P.C., Dube, G.P., and Kapuria, S., “Exact Piezoelelastic Solution of Simply-Supported Orthotropic Circular Cylindrical Panel in Cylindrical Bending”, Int. J. Solids Structure, Vol. 34 (6), pp. 685-702, (1997).

[3] Ray, M.C., Rao, K.M., and Samanta, B., “Exact Analysis of Coupled Electrostatic Behavior of a Piezoelectric Plate under Cylindrical Bending”, Compu. Struct, Vol. 45, pp. 667-677, (1992).

[4] Ray, M.C., Rao, K.M., and Samanta, B., “Exact Solution of an Intelligent Structure under Cylindrical Bending”, Compu. Struct., Vol. 47, pp. 1031-1042, (1993).

[5] Ray, M.C., Rao, K.M., and Samanta, B., “Exact Solutions for Static Analysis of Intelligent Structures”, AIAA J., Vol. 31, pp. 1684-1691, (1993).

[6] Mitchell, J.A., and Reddy, J.N., “A Study of Embedded Piezoelectric Layers in Composite Cylinders”, J. Appl. Mech., Vol. 62, pp. 162-173, (1993).

[7] Ren, J.G., “Exact Solutions for Laminated Cylindrical Shells in Cylindrical Bending”, Comp. Sci. Tech., Vol. 29, pp. 169-187, (1987).

[8] Chen, C.Q., Shen, Y.P., and Wang, X.M., “Exact Solutions for Orthotropic Cylindrical Shell with Piezoelecric Layers under Cylindrical Bending”, Int. J. Solids Struct., Vol. 33, No. 30, pp. 4481-4494, (1996).

[9] Kapuria, S., Sengupta, S., and Dumir, P.C., “Three-Dimensional Solution for Simply-Supported Piezoelectric Cylinderical Shell for Axisymmetric Load”, Compu. Methods in Appl. Mech. Eng., Vol. 29, pp. 169-187, (1997).

[10] Shakeri, M., Daneshmehr, A., and Alibiglu, A., “Elasticity Solution for Thick Laminated Shell Panel with Piezoelectric Layer”, EASEC-9 Conf., Bali, Indonesia, (2003).

[11] Shakeri, M., Alibiglu, A., and Eslami, M.R., “Elsticity Solution for Thick Laminated Anisotropic Cylindrical Panels under Dynamic Load”, J. of Mech. Eng. Sci. (ImechE), Vol. 216, part C, pp. 315-324, (2002).

[12] Tiersten, H.F., “Piezoelectric Plate Vibration”, Plenum Press, New York, pp. 54-55, (1969).

[13] Chen, C.Q., and Shen, Y.P., “Piezothermoelasticity Analysis for Cylindrical Shell under the State of Axisymmetric Deformation”, Int. J. Engng Sci., Vol. 34, No. 14, pp. 1585-1600, (1996).

Nomenclature

d: piezoelectric coefficient
$[e]$: piezoelectric constants $[C]$: the matrices of elastic constants
$\{D\}$: and the electric displacement vector
D_r: electrical displacement
$\{E\}$: the electric field vector
Y: Young's modulus

Greek symbols

$\{\sigma\}$: the stress components
$\{\varepsilon\}$: the strain components
$[\eta]$: dielectric constants of the piezoelastic material

Appendix

A.1 P.D.E operator's

$$
\begin{aligned}
L_{1r} &= C_{11}\frac{\partial^2(\ )}{\partial r^2} + \frac{C_{11}}{r}\frac{\partial(\ )}{\partial r} - \frac{C_{22}}{r^2} + \frac{C_{66}}{r^2}\frac{\partial^2(\ )}{\partial \theta^2} + C_{55}\frac{\partial^2(\ )}{\partial z^2}\\
L_{1\theta} &= -\frac{C_{22}+C_{66}}{r^2}\frac{\partial(\ )}{\partial \theta} + \frac{C_{12}+C_{66}}{r}\frac{\partial^2(\ )}{\partial \theta \partial r}\\
L_{1z} &= \frac{C_{13}-C_{23}}{r}\frac{\partial(\ )}{\partial z} + (C_{13}+C_{55})\frac{\partial^2(\ )}{\partial z \partial r}\\
L_{1\psi} &= e_{15}\frac{\partial^2(\ )}{\partial z^2} + \frac{e_{24}}{r^2}\frac{\partial^2(\ )}{\partial \theta^2} + \frac{e_{33}-e_{32}}{r}\frac{\partial(\ )}{\partial r} + e_{33}\frac{\partial^2(\ )}{\partial r^2}\\
L_{2r} &= \frac{C_{66}+C_{22}}{r^2}\frac{\partial(\ )}{\partial \theta} + \frac{C_{12}+C_{66}}{r}\frac{\partial^2(\ )}{\partial \theta \partial r}\\
L_{2\theta} &= C_{66}\frac{\partial^2(\ )}{\partial r^2} - \frac{C_{66}}{r^2} + \frac{C_{66}}{r}\frac{\partial(\ )}{\partial r} + \frac{C_{22}}{r^2}\frac{\partial^2(\ )}{\partial \theta^2} + C_{44}\frac{\partial^2(\ )}{\partial z^2}\\
L_{2z} &= \frac{C_{13}-C_{23}}{r}\frac{\partial(\ )}{\partial z} + (C_{13}+C_{55})\frac{\partial^2(\ )}{\partial z \partial r}\\
L_{2\psi} &= e_{15}\frac{\partial^2(\ )}{\partial z^2} + \frac{e_{24}}{r^2}\frac{\partial^2(\ )}{\partial \theta^2} + \frac{e_{33}-e_{32}}{r}\frac{\partial(\ )}{\partial r} + e_{33}\frac{\partial^2(\ )}{\partial r^2}
\end{aligned}
$$

$$
\begin{aligned}
L_{3r} &= \frac{C_{23}+C_{55}}{r}\frac{\partial(\ )}{\partial z} + (C_{13}+C_{55})\frac{\partial^2(\ )}{\partial z \partial r} \\
L_{3\theta} &= \frac{C_{23}+C_{55}}{r}\frac{\partial^2(\ )}{\partial z \partial \theta} \\
L_{3z} &= C_{55}\frac{\partial^2(\ )}{\partial r^2} + \frac{C_{44}}{r^2}\frac{\partial^2(\ )}{\partial \theta^2} + C_{33}\frac{\partial^2(\ )}{\partial z^2} + \frac{C_{55}}{r}\frac{\partial(\ )}{\partial r} \\
L_{3\psi} &= \frac{e_{15}}{r}\frac{\partial(\ )}{\partial z} + (e_{15}+e_{31})\frac{\partial^2(\ )}{\partial z \partial r} \\
L_{4r} &= e_{33}\frac{\partial^2(\ )}{\partial r^2} + \frac{e_{24}}{r^2}\frac{\partial^2(\ )}{\partial \theta^2} + e_{15}\frac{\partial^2(\ )}{\partial z^2} + \frac{e_{33}+e_{32}}{r}\frac{\partial(\ )}{\partial r} \\
L_{4\theta} &= -\frac{e_{24}}{r^2}\frac{\partial(\ )}{\partial \theta^2} + \frac{e_{24}+e_{32}}{r}\frac{\partial^2(\ )}{\partial \theta \partial r} \\
L_{4z} &= \frac{e_{31}}{r}\frac{\partial(\ )}{\partial r} + (e_{15}+e_{31})\frac{\partial^2(\ )}{\partial z \partial r} \\
L_{4\psi} &= -\frac{\eta_{33}}{r}\frac{\partial(\ )}{\partial r} - \eta_{33}\frac{\partial^2(\ )}{\partial r^2} - \frac{\eta_{22}}{r^2}\frac{\partial^2(\ )}{\partial \theta^2} - \eta_{11}\frac{\partial^2(\ )}{\partial z^2}
\end{aligned}
$$

A.2 O.D.E operator's

$$
\begin{aligned}
L^*_{1r} &= C_{11}\frac{\partial^2(\ )}{\partial r^2} + \frac{C_{11}}{r}\frac{\partial(\ )}{\partial r} - \frac{C_{22}}{r^2} - \frac{C_{66}}{r^2}\ b_m^2 - C_{55}\ b_n^2 \\
L^*_{1\theta} &= \frac{C_{22}+C_{66}}{r^2}\ b_m - \frac{C_{12}+C_{66}}{r}\ b_m\frac{\partial(\ )}{\partial r} \\
L^*_{1z} &= \frac{C_{23}-C_{13}}{r}\ b_n - (C_{13}+C_{55})\ b_n\frac{\partial(\ )}{\partial r} \\
L^*_{1\psi} &= -e_{15}\ b_n^2 - \frac{e_{24}}{r^2}\ b_m^2 - \frac{e_{32}-e_{33}}{r}\frac{\partial(\ )}{\partial r} + e_{33}\frac{\partial^2(\ )}{\partial r^2} \\
L^*_{2r} &= \frac{C_{66}+C_{22}}{r^2}\ b_m + \frac{C_{12}+C_{66}}{r}\ b_m\frac{\partial(\ )}{\partial r} \\
L^*_{2\theta} &= C_{66}\frac{\partial^2(\ )}{\partial r^2} - \frac{C_{66}}{r^2} + \frac{C_{66}}{r}\frac{\partial(\ )}{\partial r} - \frac{C_{22}}{r^2}b_m^2 - C_{44}b_n^2 \\
L^*_{2z} &= -\frac{C_{23}}{r}\ b_m b_n - \frac{C_{44}}{r}\ b_m b_n \\
L^*_{2\psi} &= \frac{e_{24}+e_{32}}{r}\ b_m\frac{\partial(\ )}{\partial r} + \frac{e_{24}}{r^2}\ b_m \\
L^*_{3r} &= \frac{C_{23}+C_{55}}{r}\ b_n + (C_{13}+C_{55})\ b_n\frac{\partial(\ )}{\partial r} \\
L^*_{3\theta} &= -\frac{C_{23}}{r}\ b_m b_n - \frac{C_{44}}{r}\ b_m b_n \\
L^*_{3z} &= C_{55}\frac{\partial^2(\ )}{\partial r^2} + \frac{C_{55}}{r}\frac{\partial(\ )}{\partial r} - \frac{C_{44}}{r^2}b_m^2 - C_{33}b_n^2 \\
L^*_{3\psi} &= (e_{15}+e_{31})\ b_n\frac{\partial(\ )}{\partial r} + \frac{e_{15}}{r}\ b_n
\end{aligned}
$$

$$L^*_{4r} = e_{33}\frac{\partial^2(\ )}{\partial r^2} - \frac{e_{24}}{r^2}b_m^2 - e_{15}b_n^2 + \frac{e_{33}+e_{32}}{r}\frac{\partial(\ )}{\partial r}$$
$$L^*_{4\theta} = \frac{e_{24}}{r^2}\ b_m - \frac{e_{24}+e_{32}}{r}\ b_m\frac{\partial(\ )}{\partial r}$$
$$L^*_{4z} = -\frac{e_{31}}{r}\ b_n - (e_{15}+e_{31})\ b_n\frac{\partial(\ )}{\partial r}$$
$$L^*_{4\psi} = -\frac{\eta_{33}}{r}\frac{\partial(\ )}{\partial r} - \eta_{33}\frac{\partial^2(\ )}{\partial r^2} + \frac{\eta_{22}}{r^2}\ b_m^2 + \eta_{11}b_n^2$$

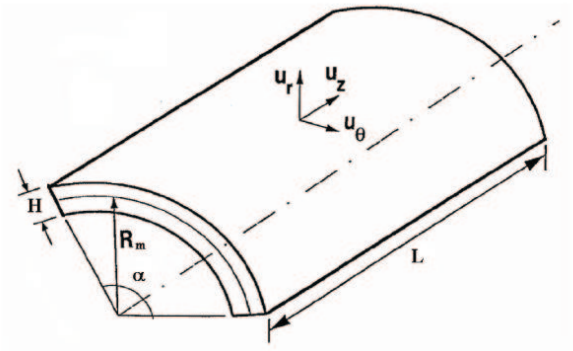

Figure 1 geometry of panel.

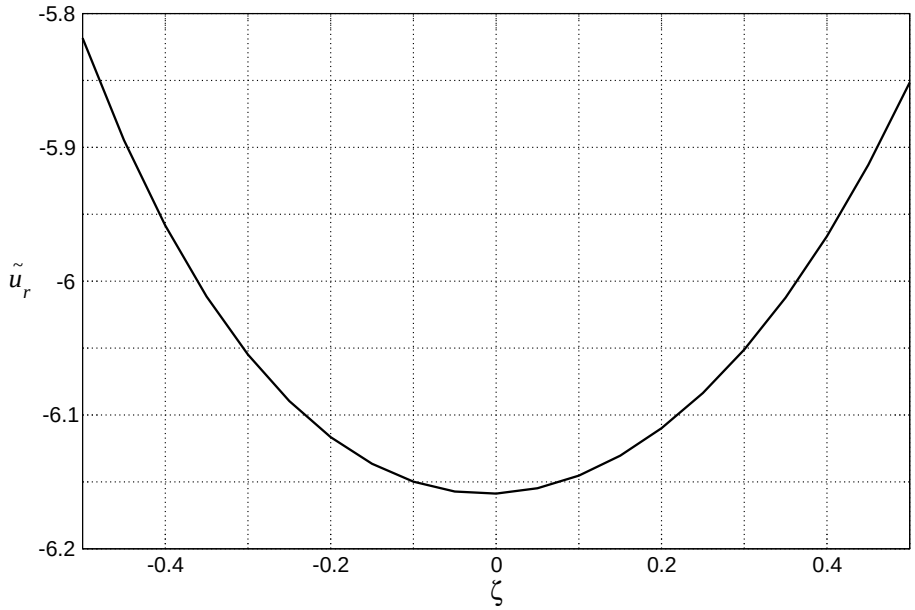

Figure 2 Distribution of $\tilde{u}_r(\alpha/2, L/2)$ for panel with $S = 4$ and outer sinusoidal pressure versus dimensionless thickness (ζ).

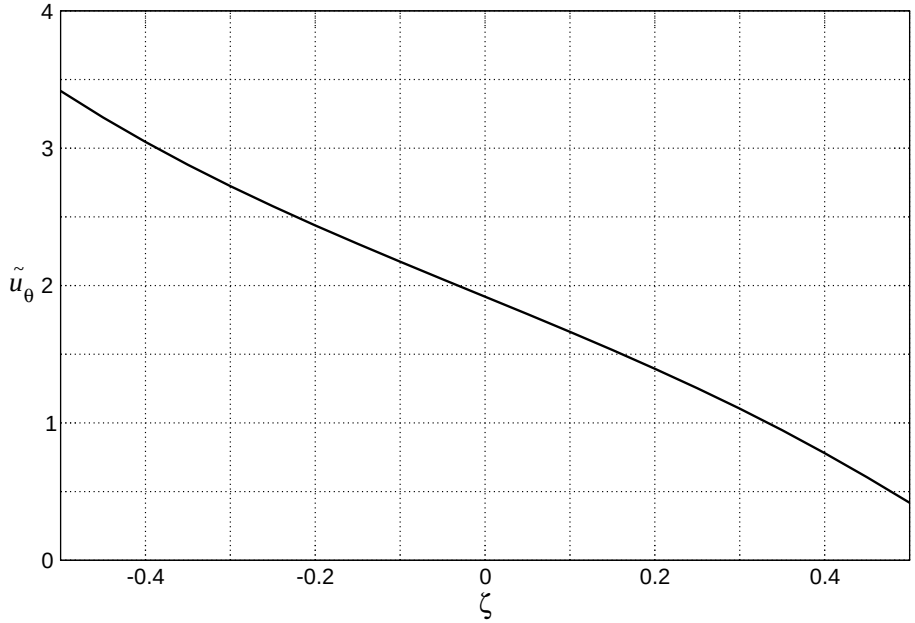

Figure 3 Distribution of $\tilde{u}_\theta(0, L/2)$ for panel with $S = 4$ and outer sinusoidal pressure versus dimensionless thickness (ζ).

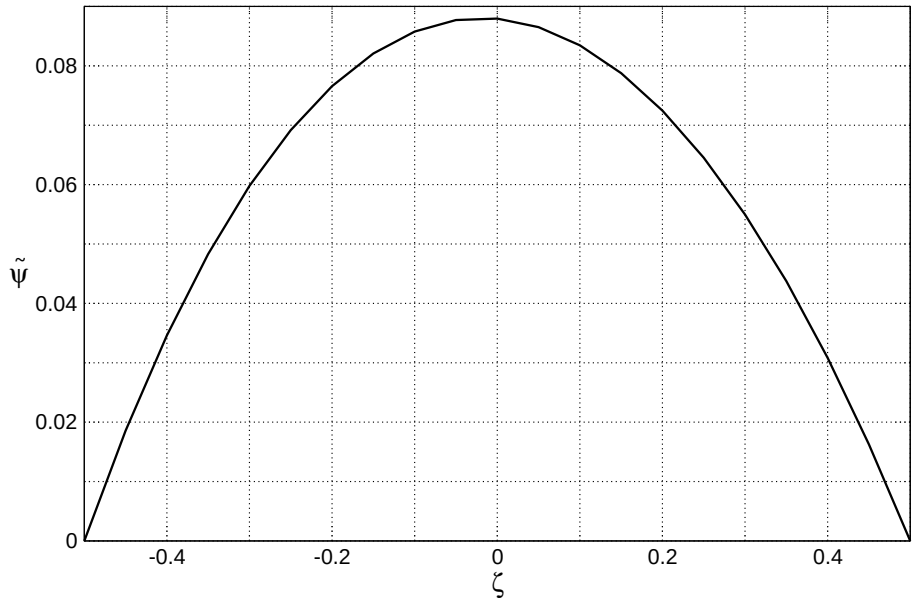

Figure 4 Distribution of $\tilde{\psi}(\alpha/2, L/2)$ for panel with $S = 4$ and outer sinusoidal pressure versus dimensionless thickness (ζ).

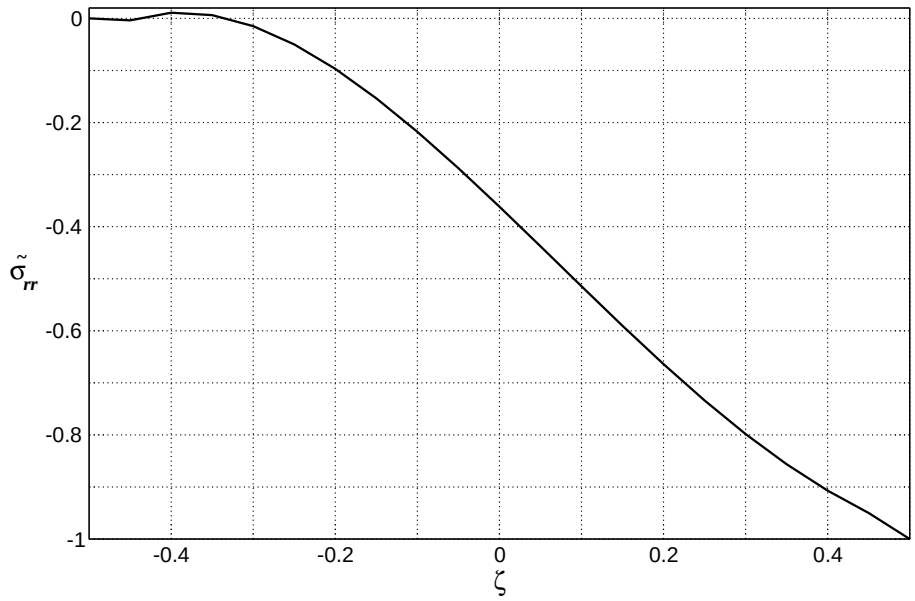

Figure 5 Distribution of $\tilde{\sigma}_{rr}(\alpha/2, L/2)$ for panel with $S = 4$ and outer sinusoidal pressure versus dimensionless thickness (ζ).

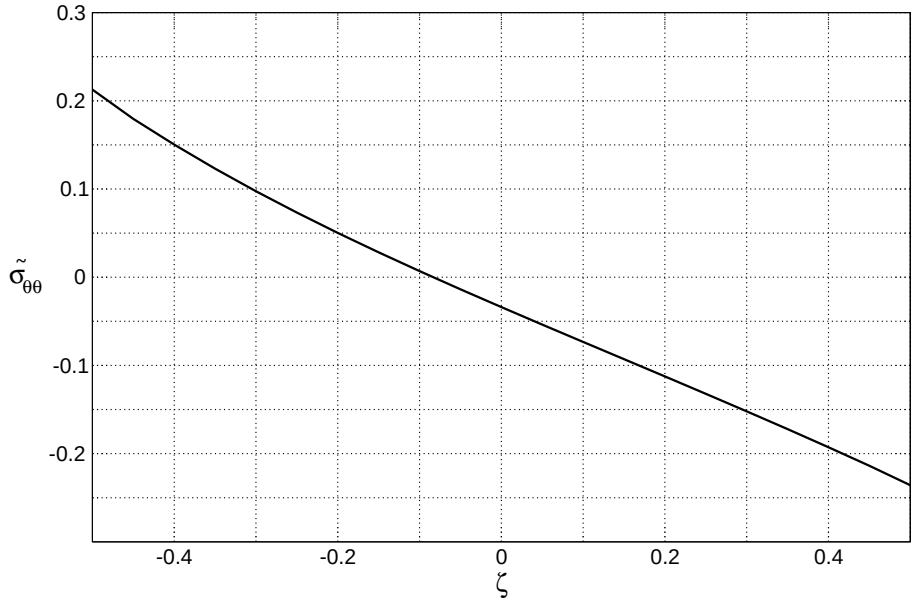

Figure 6 Distribution of $\tilde{\sigma}_{\theta\theta}(\alpha/2, L/2)$ for panel with $S = 4$ and outer sinusoidal pressure versus dimensionless thickness (ζ).

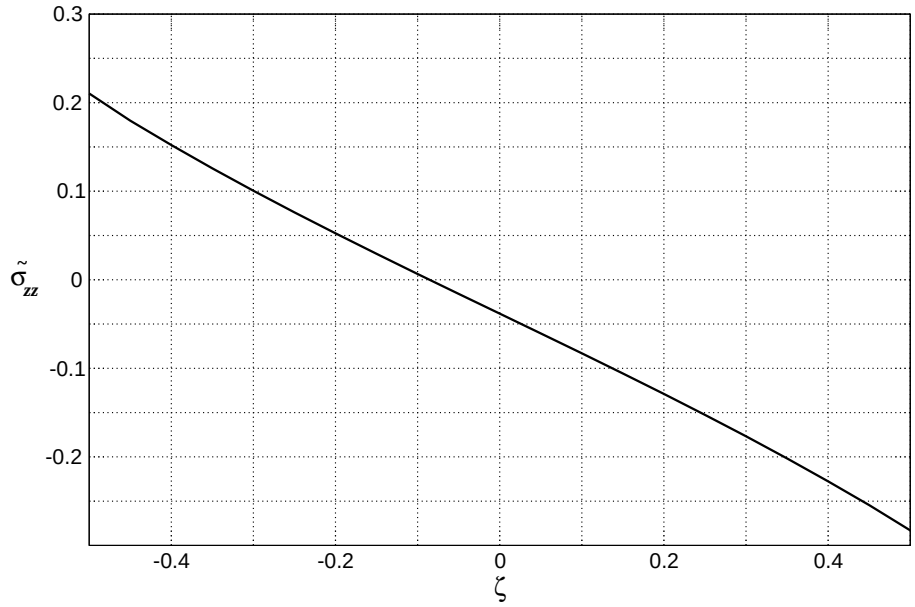

Figure 7 Distribution of $\tilde{\sigma}_{zz}(\alpha/2, L/2)$ for panel with $S = 4$ and outer sinusoidal pressure versus dimensionless thickness (ζ).

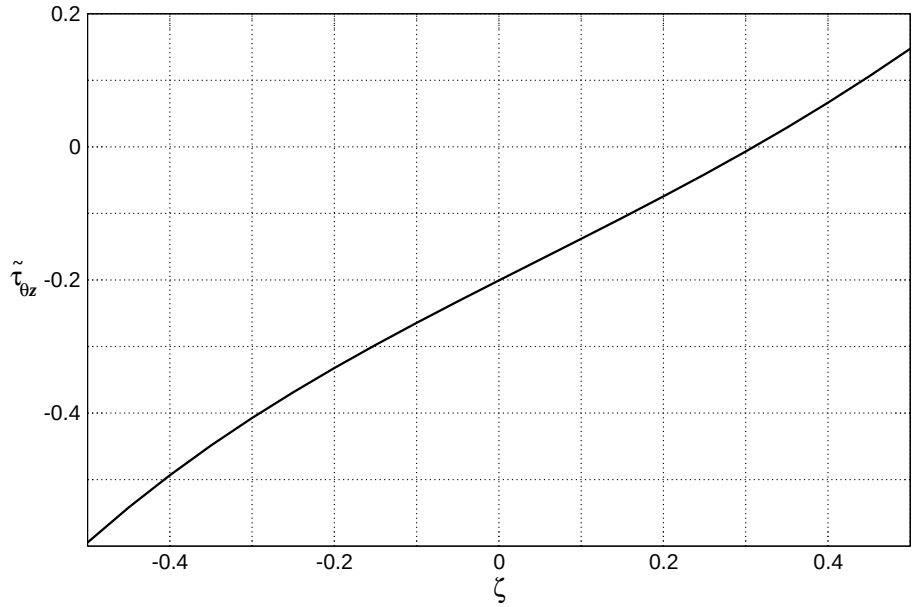

Figure 8 Distribution of $\tilde{\tau}_{\theta z}(0, L)$ for panel with $S = 4$ and outer sinusoidal pressure versus dimensionless thickness (ζ).

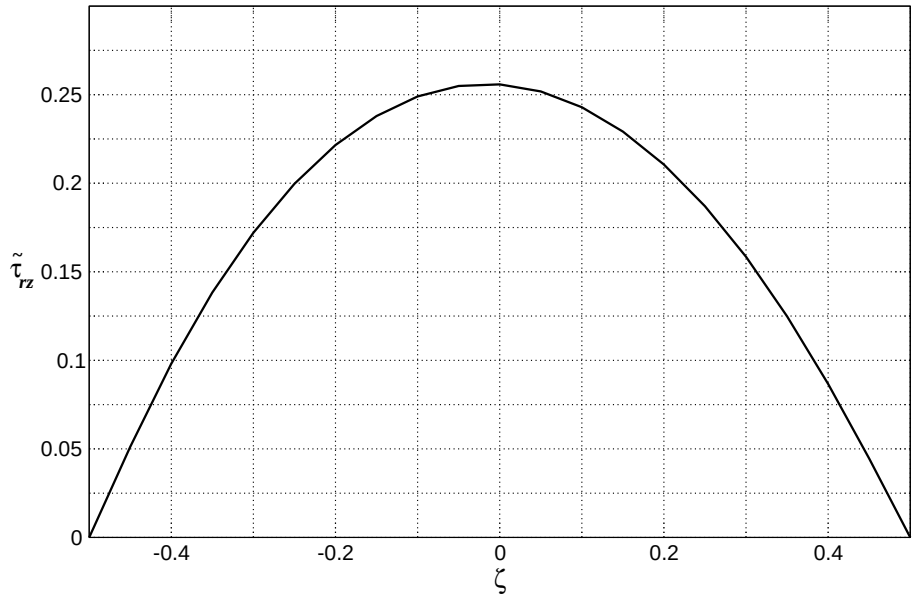

Figure 9 Distribution of $\tilde{\tau}_{rz}(\alpha/2, L)$ for panel with $S = 4$ and outer sinusoidal pressure versus dimensionless thickness (ζ).

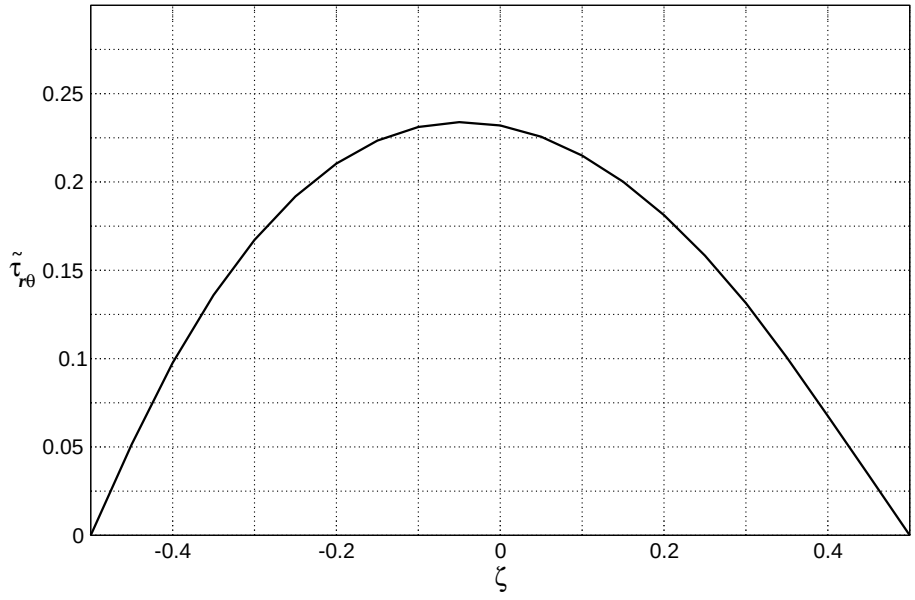

Figure 10 Distribution of $\tilde{\tau}_{r\theta}(0, L/2)$ for panel with $S = 4$ and outer sinusoidal pressure versus dimensionless thickness (ζ).